

Chapter 10

Formation and evolution of the Local Group

480 Myr < t < 13.7 Gyr; $10 > z > 0$; 30 K > T > 2.725 K

The fact that the [G]alactic system is a member of a group is a very fortunate accident.

Edwin Hubble, The Realm of the Nebulae

Summary: The Local Group (LG) is the group of galaxies gravitationally associated with the Galaxy and M 31. Galaxies within the LG have overcome the general expansion of the universe. There are approximately 75 galaxies in the LG within a diameter of ~ 3 Mpc having a total mass of $2\text{--}5 \times 10^{12} M_{\odot}$. A strong morphology-density relation exists in which gas-poor dwarf spheroidals (dSphs) are preferentially found closer to the Galaxy/M 31 than gas-rich dwarf irregulars (dIrrs). This is often promoted as evidence of environmental processes due to the massive Galaxy and M 31 driving the evolutionary change between dwarf galaxy types. High Velocity Clouds (HVCs) are likely to be either remnant gas left over from the formation of the Galaxy, or associated with other galaxies that have been tidally disturbed by the Galaxy. Our Galaxy halo is about 12 Gyr old. A thin disk with ongoing star formation and older thick disk built by $z \geq 2$ minor mergers exist. The Galaxy and M 31 will merge in 5.9 Gyr and ultimately resemble an elliptical galaxy. The LG has $v_{LG} = 627 \pm 22 \text{ km s}^{-1}$ with respect to the CMB. About 44% of the LG motion is due to the infall into the region of the Great Attractor, and the remaining amount of motion is due to more distant overdensities between 130 and 180 h^{-1} Mpc, primarily the Shapley supercluster.

Learning objectives: By reading this chapter you will learn about:

10.1 The components of the Local Group

10.2 Formation of the Local Group

10.3 Dynamical estimates of the Local Group mass

10.4 The use of the Local Group as a laboratory

10.5 The components of the Galaxy

10.6 Formation and evolution of the Galaxy

10.7 The future of the Local Group

This chapter describes the Local Group (LG) of galaxies, in particular the formation and evolution of the LG based on the stellar properties and kinematics of group members. The Galaxy and the Andromeda galaxy, M 31 dominate the Local Group, with the LG barycentre approximately half way between the two galaxies. The LG contains over 70 galaxies in a region of space with a diameter of 3 Mpc, most of which are relatively low luminosity dwarfs. The LG is part of the Local Supercluster (see also Section 1.1.7). The chemical, dynamical and structural properties of the Galaxy are described. The likely formation scenario of the Galaxy is presented. We finish the chapter by describing the future evolution of the LG. It will approach the Virgo cluster but never reach it, as the accelerated expansion of the universe determines its ultimate, isolated state.

10.1 Local Group

The imaginatively (!) named Local Group (LG) is the group of galaxies gravitationally associated with the two large galaxies, the Galaxy and M 31. Galaxies within the LG have overcome the general expansion of the universe. There are approximately 75 galaxies (McConnachie 2012) in the LG that has a diameter of ~ 3 Mpc and a total mass of $2\text{--}5 \times 10^{12} M_{\odot}$. The number of members is expected to increase as new sky surveys (i.e. SkyMapper, Large Synoptic Survey Telescope) begin to provide better imaging capabilities. It is likely that other potential members are hidden by dust and gas close to the plane of the Galaxy.

Table 10.1 uses information from McConnachie (2012) and lists 75 galaxies with $D_{LG} < 1330$ kpc. This measure, D_{LG} is the distance to the barycentre of the LG, assumed to be the mid-point of the line joining the Galaxy and M 31. The table also lists galaxy type, absolute magnitude in V, Galactic longitude and latitude, distance modulus and v_{LG} , the velocity of the galaxy relative to the barycentre position of the LG. The zero-velocity surface of the LG (with the radius $R_{LG} = 1060 \pm 70$ kpc) is taken to be the mean distance of the galaxies WLM, Leo A, Aquarius, Tucana, SagDIG (see Figure 10.1) and UGC 4879, that cluster around a velocity of $v_{LG} = 0$ km s⁻¹. The LG is part of the Virgo (or Local) Supercluster.

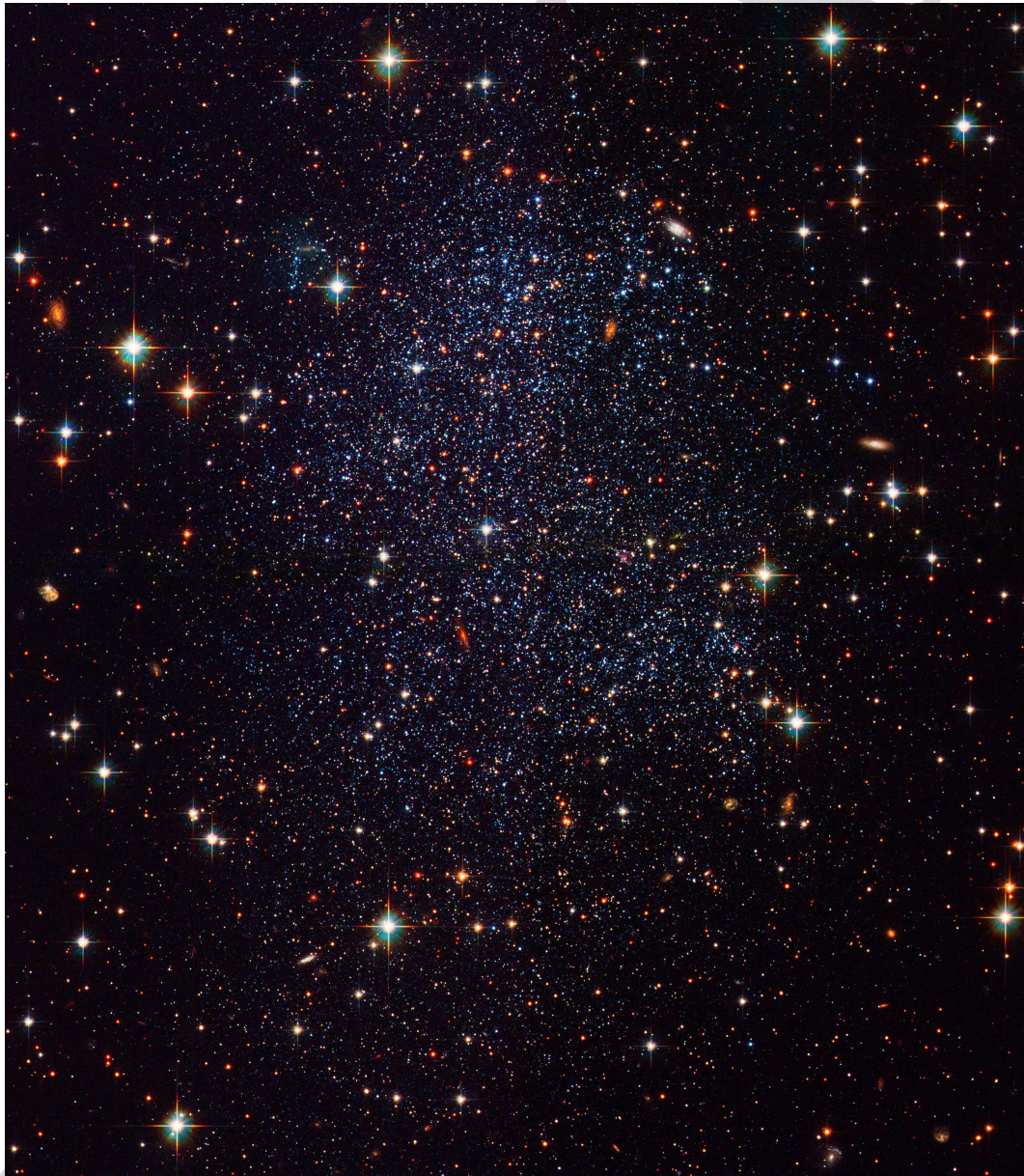


Figure 10.1: The Local Group member Sagittarius Dwarf Irregular galaxy (SagDIG), at a distance 1.1 Mpc, observed by HST ACS in F435W (B), F606W (V) and F814W (I). Credit: NASA, ESA, and Y. Momany (University of Padua)

The Local Group

Name	Type	M_V	Gal. Long. ℓ	Gal. Lat. b	$(m-M)_0$	D_{LG} (kpc)	v_{LG} (km s $^{-1}$)
The Galaxy	S(B)bc						
Canis Major	?	-14.4	240.0	-8.0	14.29	394	-172
Sagittarius dSph	dSph	-13.5	5.6	-14.2	17.10	400	159
Segue (I)	dSph	-1.5	220.5	+50.4	16.80	401	69
Ursa Major II	dSph	-4.2	152.5	+37.4	17.50	380	-3
Bootes II	dSph	-2.7	353.7	+68.9	18.10	416	-156
Segue II	dSph	-2.5	149.4	-38.1	17.70	361	112
Willman 1	dSph	-2.7	158.6	+56.8	17.90	390	41
Coma Berenices	dSph	-4.1	241.9	+83.6	18.20	412	46
Bootes III	dSph?	-5.8	35.4	+75.4	18.35	410	219
LMC	Irr	-18.1	280.5	-32.9	18.52	421	12
SMC	dIrr	-16.8	302.8	-44.3	19.03	422	-35
Bootes (I)	dSph	-6.3	358.1	+69.6	19.11	430	69
Draco	dSph	-8.8	86.4	+34.7	19.40	366	-46
Ursa Minor	dSph	-8.8	105.0	+44.8	19.40	370	-44
Sculptor	dSph	-11.1	287.5	-83.2	19.67	379	97
Sextans (I)	dSph	-9.3	243.5	+42.3	19.67	450	6
Ursa Major (I)	dSph	-5.5	159.4	+54.4	19.93	391	0
Carina	dSph	-9.1	260.1	-22.2	20.11	454	-53
Hercules	dSph	-6.6	28.7	+36.9	20.60	444	141
Fornax	dSph	-13.4	237.1	-65.7	20.84	394	-30
Leo IV	dSph	-5.8	264.4	+57.4	20.94	513	-54
Canes Venatici II	dSph	-4.9	113.6	+82.7	21.02	458	-113
Leo V	dSph	-5.2	261.9	+58.5	21.25	530	-7
Pisces II	dSph	-5.0	79.2	-47.1	21.30:	285	...
Canes Venatici (I)	dSph	-8.6	74.3	+79.8	21.69	493	62
Leo II	dSph	-9.8	220.2	+67.2	21.84	529	-16
Leo I	dSph	-12.0	226.0	+49.1	22.02	551	125
Andromeda	Sb	-21.0	121.2	-21.6	24.47	392	-34
M 32	cE	-16.4	121.2	-22.0	24.53	414	67
Andromeda IX	dSph	-8.1	123.2	-19.7	24.42	375	56
NGC 205	dE/dSph	-16.5	120.7	-21.1	24.58	433	22
Andromeda XVII	dSph	-8.7	120.2	-18.5	24.50	404	...
Andromeda I	dSph	-11.7	121.7	-24.8	24.36	355	-116
Andromeda XXVII	dSph	-7.9	120.4	-17.4	24.59	439	...
Andromeda III	dSph	-10.0	119.4	-26.3	24.37	360	-83
Andromeda XXV	dSph	-9.7	119.2	-15.9	24.55	426	...
Andromeda XXVI	dSph	-7.1	118.1	-14.7	24.41	377	...
Andromeda XI	dSph	-6.9	121.7	-29.1	24.40	374	-167
Andromeda V	dSph	-9.1	126.2	-15.1	24.44	389	-143

The Local Group, continued

Name	Type	M_V	Gal. Long. ℓ	Gal. Lat. b	$(m-M)_0$	D_{LG} (kpc)	v_{LG} (km s $^{-1}$)
Andromeda X	dSph	-7.6	125.8	-18.0	24.23	314	95
Andromeda XXIII	dSph	-10.2	131.0	-23.6	24.43	388	...
Andromeda XX	dSph	-6.3	112.9	-26.9	24.52	420	...
Andromeda XII	dSph	-6.4	122.0	-28.5	24.70	485	-306
NGC 147	dE/dSph	-14.6	119.8	-14.3	24.15	292	85
Andromeda XXI	dSph	-9.9	111.9	-19.2	24.67	476	...
Andromeda XIV	dSph	-8.4	123.0	-33.2	24.33	361	-240
Andromeda XV	dSph	-9.4	127.9	-24.5	24.00	247	-95
Andromeda XIII	dSph	-6.7	123.0	-29.9	24.80	528	53
Andromeda II	dSph	-12.4	128.9	-29.2	24.07	276	40
NGC 185	dE/dSph	-14.8	120.8	-14.5	23.95	234	72
Andromeda XXIX	dSph	-8.3	109.8	-30.8	24.32	363	...
Andromeda XIX	dSph	-9.2	115.6	-27.4	24.85	548	...
Triangulum	Sc	-18.8	133.6	-31.3	24.54	442	37
Andromeda XXIV	dSph	-7.6	127.8	-16.3	23.89	220	...
Andromeda VII	dSph	-12.6	109.5	-10.0	24.41	401	-8
Andromeda XXII	dSph	-6.5	132.6	-34.1	24.50:	432	...
IC 10	dIrr	-15.0	119.0	-3.3	24.50	440	-64
LGS 3	dIrr/dSph	-10.1	126.8	-40.9	24.43	422	-74
Andromeda VI	dSph	-11.3	106.0	-36.3	24.47	435	-93
Andromeda XVI	dSph	-9.2	124.9	-30.5	23.60	153	-143
Andromeda XXVIII	dSph?	-8.5	91.0	-22.9	24.10	364	...
IC 1613	dIrr	-15.2	129.7	-60.6	24.39	517	-90
Phoenix	dIrr/dSph	-11.2	272.2	-68.9	23.09	556	-106
NGC 6822	dIrr	-15.2	25.4	-18.4	23.31	595	64
Cetus	dSph	-11.2	101.5	-72.9	24.39	603	26
Pegasus dIrr	dIrr/dSph	-12.2	94.8	-43.6	24.82	618	60
Leo T	dIrr/dSph	-8.0	214.9	+43.7	23.10	651	-98
WLM	dIrr	-14.2	75.9	-73.6	24.85	794	-24
Leo A	dIrr	-12.1	196.9	+52.4	24.51	941	-41
Andromeda XVIII	dSph	-9.7	113.9	-16.9	25.66	969	...
Aquarius	dIrr/dSph	-10.6	34.0	-31.3	25.15	1053	9
Tucana	dSph	-9.5	322.9	-47.4	24.74	1076	73
Sagittarius dIrr	dIrr	-11.5	21.1	-16.3	25.14	1156	22
UGC 4879	dIrr/dSph	-12.5	164.7	+42.9	25.67	1321	-12

Notes

- The above table is based on Tables 1, 2 and 3 of McConnachie (2012). M_V for M 31 is calculated from the table value above of $(m-M)_0$ and $V=3.44$ (Gil de Paz 2007).

The LG is dominated by the Galaxy and the type Sb galaxy M 31, the Andromeda galaxy with $M_V \sim -20$. Recent revisions (Brunthaler *et al.* 2011) of the rotation velocity (Θ_0) of the Galaxy using radio VLBI measurements suggest that our Galaxy is at least as massive as M 31. The Galaxy and M 31 are approaching each other at $\sim 120 \text{ km s}^{-1}$. The next dominant galaxy is M 33 ($M_V \sim -18.8$) in Triangulum, belonging to the M 31 subsystem of galaxies, and is about 20% as luminous as the Galaxy.

Nearer to the Galaxy are the well known Large and Small Magellanic Clouds (LMC and SMC respectively). The LMC is 50 kpc distant, and the SMC slightly further at 61 kpc. Even closer are Canis Major ($D_{MW} = 13 \text{ kpc}$) and the Sagittarius dSph ($D_{MW} = 18 \text{ kpc}$), the two closest of nine galaxies between the Galaxy and the distance of the LMC. M 32, a close companion to M 31 is the only elliptical in the LG, with $M_V \sim -16.4$. It has an unusually high central stellar concentration and is classified cE, with the 'c' denoting compact.

McConnachie (2012) considers all galaxies with absolute magnitude fainter than $M_V \sim -18$, to be classified as dwarfs. Hence the vast majority of galaxies listed in Table 10.1 are classified as dwarfs, and 53 out of 75 galaxies are classified as dwarf spheroidal (dSph). Many of these dSphs are satellites of the Galaxy or M 31.

There are a number of nearby groups of galaxies to the LG. These include the NGC 3109 ($D \sim 1.3 \text{ Mpc}$), NGC 55 ($\sim 2.2 \text{ Mpc}$), IC 342/Maffei ($\sim 3.3 \text{ Mpc}$), M 81 ($\sim 3.6 \text{ Mpc}$), Centaurus A ($\sim 3.7 \text{ Mpc}$), Sculptor ($\sim 3.9 \text{ Mpc}$) and Canes Venatici I/M 94 ($\sim 4.5 \text{ Mpc}$) groups.

van den Bergh (2000) derived a Local Group velocity dispersion $\sigma_r = 61 \pm 8 \text{ km s}^{-1}$ and uses

$$\langle \sigma^2 \rangle \simeq 0.4 \frac{GM}{R_h} \quad (10.1)$$

(from page 217 of Binney and Tremaine 1987), that assumes the Virial Theorem and isotropic motions such that $\langle \sigma \rangle = 3\langle \sigma_r \rangle$. Adopting the radius in which half the mass is enclosed, $R_h = 350 \text{ kpc}$ yields a Local Group mass of $2.3 \pm 0.6 \times 10^{12} M_\odot$. Karachentsev and Kashibadze (2006) derive the radii of the zero-velocity sphere of the LG to be $R_{LG} = 0.96 \text{ Mpc}$ yielding a smaller mass of the LG = $1.3 \times 10^{12} M_\odot$.

- Our Galaxy resides in the Local Group which contains more than 70 galaxies. The Galaxy and the Andromeda galaxy M 31 dominate the Local Group, which has overcome the general expansion of the universe.

10.1.1 Formation of the Local Group

Studies to determine the possible formation and evolution of the LG over a 13.7 Gyr timescale are of course subject to many uncertainties. It is usually assumed that the Galaxy and M 31 formed nearby to each other, and took part in the general expansion of the universe. Around 4 Gyr ago, their mutual gravitational attraction overcame the general expansion and they began to approach each other. At present they are ~ 750 kpc apart and approaching at ~ 120 km s $^{-1}$. Formation models that only consider the two major galaxies in the LG are of course an oversimplification. The relative motions and distances of other LG members can be used to constrain the validity of this simplified model as described below and is a factor when deriving the dynamically-based mass of the LG (as in Section 10.1.2) and is further discussed in Section 10.1.3.

Peebles, Tully and Shaya (2011) have produced a dynamical model of 28 galaxies (including the Galaxy) currently within 1.5 Mpc. The model does not show the assumed previous interaction between M 31 and M 33 (as suggested by the stellar and gaseous properties of the two galaxies and discussed shortly in Section 10.2.1). However it suggests that 10 LG galaxies originate from a common direction (possibly from a failed assembly of a larger galaxy), and that NGC 6822 was in close proximity to the Galaxy at $z \sim 0.27$. Their dynamical model begins at $z = 9$ and assumes that any original peculiar velocities are smaller than present values.

In Figure 10.2 the predicted orbits of 5 galaxies relative to the Galaxy (red central dot) are shown.

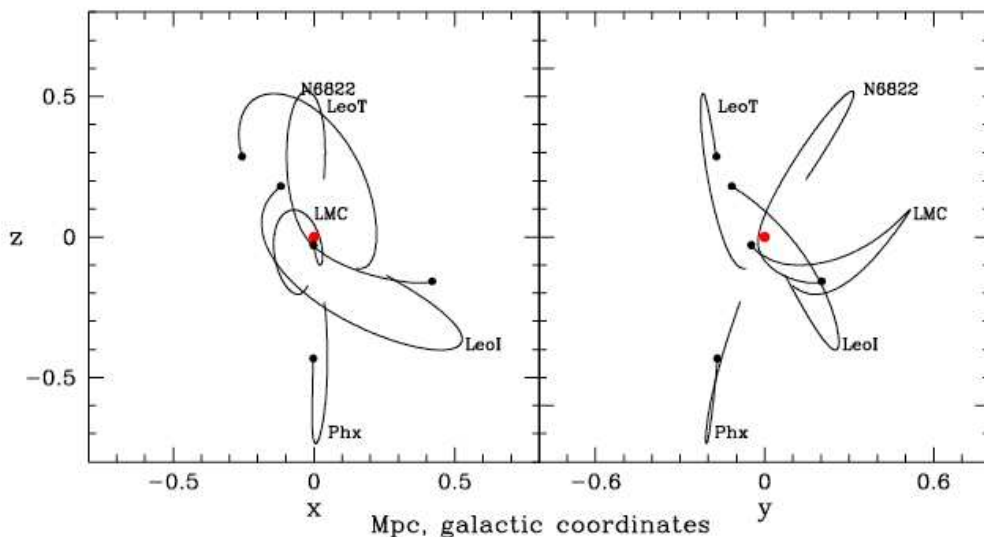


Figure 10.2: Predicted galaxy orbits, relative to the Galaxy (red central dot), from $z = 1$ (near each label) to present (black dots). Credit: Peebles, Tully and Shaya (2011)

The orbits are traced from $z = 1$ (near each label) to their present position (black dots). The close passage of NGC 6822 is clearly indicated. The orbit of the Large Magellanic Cloud (LMC) is shown, but the Small Magellanic Cloud is excluded from the model since it may be interacting with the LMC. Leo T and Phoenix are approaching the Galaxy for the first time. Leo I had a closest approach of 200 kpc, and the lack of H I in the galaxy suggests that ram pressure may have been enough to remove any gas. NGC 6822 came even closer, 34 kpc, to the Galaxy, and that whilst no tidal tail (similar to the Magellanic Stream) is evident, the authors note that the distribution of H I extends along the major (long) axis, not in a way normally expected for an isolated rotating gas disk.

Interestingly, fitting the LG galaxy positions and velocities in the model implies a larger circular velocity of 256 km s^{-1} for the rotation of the Galaxy than typically used ($\Theta_0 = 220 \text{ km s}^{-1}$), although it is even somewhat larger than a suggested revised velocity (239 km s^{-1}) as discussed below in Section 10.2.3.

As discussed more fully in Section 10.2.2 Tolstoy, Hill and Tosi (2009) state how all dwarf galaxies in the LG possess old ($>10 \text{ Gyr}$) stars. van den Bergh (2003) shows that almost all LG galaxies have RR Lyrae variables, suggestive of 10 Gyr old populations. As well he suggests that the oldest globular clusters formed out of halo gas shocked by ionization fronts generated during cosmic reionization at $5 < z < 15$. Weinmann *et al.* (2007) studied the dependence of reionization history with halo mass and environment. They find that halos less massive than the transition mass of $\sim 10^{12} M_\odot$, are likely to be reionized by distant sources. Higher mass halos form earlier than lower mass halos, and are reionized earlier, typically by internal sources.

Cosmological simulations can provide valuable information on the assembly of dark matter halos in the early universe which directly contribute to the way the baryonic structures have formed and evolved. The assembly of the LG in a Λ CDM cosmological model, is studied in Forero-Romero *et al.* (2011). The build up of mass via the assembly of dark halos is characterised by the mass aggregation history (MAH). For the purpose of the study, the resultant LG is defined as having two basic elements. The masses of the halos should match the present day Galaxy and M 31 halos, and that these two halos be isolated from other massive halos. Three N-body simulations are used to identify potential LGs, that mimic the two main halos (within a specific halo mass range of $5 \times 10^{11} M_\odot < M_h < 5 \times 10^{12} M_\odot$ at $z = 0$) of the Galaxy and M 31, and reproduce the relative distance between the LG and the Virgo cluster.

Each of the three simulations suggests that the LG underwent a major merger (with a minimal mass ratio of 10:1) on average $\sim 10\text{-}12 \text{ Gyr}$ ago. This 'quiet' MAH is consistent with the known disk morphologies of both the Galaxy and M 31. The proposed timing of a last major merger in the Galaxy dark matter halo agrees with the existence of the predominantly old thick disk (see Section 10.4.5) produced *in*

situ by a gas-rich merger. The LG, however, may be a special or statistically unusual environment as only 1-3% of halo pairs within a mass range applicable to the LG display an appropriately 'quiet' MAH.

10.1.2 Mass of the Local Group

Kahn and Woltjer (1959) determined the mass of the LG from a method called "Local Group Timing". Using Keplers' 3rd law and the conservation of energy, they find a dynamical mass at least 4 times larger than the individual masses of the Galaxy and M 31. The authors then made a case for the existence of intergalactic matter mainly in the form of gas, to make up the mass shortfall. We now consider most of this shortfall to be predominantly dark matter.

A study (van der Marel and Guhathakurta 2008) of the relative motions of the Galaxy and M 31 and of the kinematics of satellite galaxies derived the *total* mass of the LG to be between $1.7 - 5.6 \times 10^{12} M_{\odot}$. In a more recent study, van der Marel *et al.* (2012a) have used proper motion measurements of three fields in M 31 to determine its velocity vector with respect to the Galaxy. They determine a radial velocity $v_{rad,M\ 31} = -109.3 \text{ km s}^{-1}$ and a tangential velocity $v_{tan,M\ 31} = 17.0 \pm 4.4 \text{ km s}^{-1}$ consistent with a future head-on collision with the Galaxy.

The relatively small value of $v_{tan,M\ 31}$ is consistent with a lack of any significant tidal torque from nearby large-scale structure prior to radial expansion due to the Big Bang. The value is smaller than the median tangential velocity of galaxy pairs in the Λ CDM Millennium simulation (Li and White 2008), that found 24% of pairs having $v_{tan} < 50 \text{ km s}^{-1}$. Combined with a 'quiet' MAH, this low tangential velocity $v_{tan,M\ 31}$ may suggest the LG is a special case of a galaxy group.

van der Marel *et al.* (2012a) find a LG timing (virial) mass, of

$$M_{tot,vir} \equiv M_{MW,vir} + M_{M\ 31,vir} = 4.9 \times 10^{12} M_{\odot} \quad (10.2)$$

with an uncertainty of 32%. The virial mass is the mass enclosed within the virial radius, as given by (see Appendix 1 of van der Marel *et al.* 2012a)

$$r_{vir} = 206 h^{-1} \text{ kpc} \left(\frac{\Delta_{vir} \Omega_m}{97.2} \right)^{-1/3} \left(\frac{M_{vir}}{10^{12} h^{-1} M_{\odot}} \right)^{1/3} \quad (10.3)$$

where van der Marel *et al.* (2012a) adopts $h = 0.7$ and $\Omega_m = 0.27$, that requires $\Delta_{vir} = 360$.

In comparison the individual, total masses of the MW (Wilkinson and Evans 1999) and M 31 (Evans and Wilkinson 2000) are respectively

$$M_{MW} \sim 19_{-17}^{+36} \times 10^{11} M_{\odot} \quad (10.4)$$

and

$$M_{M\ 31} \sim 12.3_{-6}^{+18} \times 10^{11} M_{\odot} \quad (10.5)$$

These total masses, slightly lower than that found by van der Marel *et al.* (2012a), are derived from the positions and radial velocities of satellite galaxies, globular clusters and planetary nebulae. Whilst the errors are large the advantage of this technique is that it determines the mass distribution at much larger radii (~ 90 kpc), than gas rotation curves, that typically extend to 30 kpc.

10.1.3 Possible interactions

The validity of the Local Group Timing method, a two-body approximation, breaks down if other galaxies of significant mass have interacted or orbited either of the Galaxy or M 31. Valtonen *et al.* (1993) speculate on past orbital interactions between IC 342 and Maffei 1 and M 31 based on their derived (nearby) distances and observed velocities.

Fingerhut *et al.* (2007) describe accurate extinction and distance estimates that place Maffei 1 and IC 342 at a distance of 3.0 Mpc, and along with Maffei 2, these three galaxies are the dominant members of the compact IC 342/Maffei group of galaxies. This revised (larger) distance than found by Valtonen *et al.* suggests it is highly unlikely that IC 342 and Maffei 1 had ever interacted with M 31.

10.1.4 New members of the Local Group

From 1940 onwards, the number of LG members has grown by about four galaxies per decade (van den Bergh 2000). Table 2.1 of van den Bergh (2000) lists 35 probable members of the LG, suggesting an even more rapid increase in detecting LG members since 2000. The increase is due to advances in observational techniques (deep, multi-colour, wide field imaging) plus improved software analysis of dense star fields, combined with an improved knowledge of where to look for potential members (e.g. near M 31) and galaxies in the process of merging with our Galaxy (e.g. Canis Major and Sagittarius dSph, see Section 10.4.2).

Some of the more recent discoveries since 1990 include:

Sextans dIrr: A dwarf elliptical galaxy at a distance of 85 kpc has been found in the constellation of Sextans (Irwin *et al.* 1990). The discovery was made from APM

measures of UK Schmidt atlas glass copy IIIaJ survey plates.

Tucana dSph: Lavery (1990) and Lavery and Mighell (1992) discovered a dwarf galaxy in Tucana. The system is highly flattened and it is classified as dE5. Tucana and five other galaxies define the zero-velocity surface of the LG (with the radius $R_{LG} = 1060 \pm 70$ kpc).

Sagittarius dSph: Ibata, Gilmore and Irwin (1994) detected an extended group of comoving stars in the direction of the Galactic Centre. It is comparable in size and luminosity to the Fornax dSph. It is elongated along the plane of the Milky Way, suggesting that it is undergoing some tidal disruption. For more see Section 10.4.2 and Figure 10.13.

Antlia dIrr: Whiting, Irwin and Hau (1997) rediscovered a dIrr in the constellation of Antlia. It is in a relatively isolated part of the Local Group, but only 1.2° away from the Local Group dwarf NGC 3109, and may be an associated system.

Andromeda V dSph: Armandroff, Davies and Jacoby (1998) used a digital filtering technique applied to 1550 deg^2 of the second Palomar Sky Survey to detect a new dSph companion to M 31.

Andromeda VII/Casseopia dSph; Andromeda VI/Pegasus dSph: Karachentsev and Karachentseva (1999) detected the Cassiopeia and Pegasus dSphs in the vicinity of M 31 on the POSS-II film copies.

Segue (I) dSph, Coma Berenices dSph, Hercules dSph, and Leo IV dSph: Belokurov *et al.* (2007) used SDSS imaging data to discover the nearby dSphs Segue (I), Coma Berenices, Hercules, and Leo IV.

Andromeda XVIII dSph, Andromeda XIX dSph, Andromeda XX dSph: McConnachie *et al.* (2008) detected 3 dSphs. Andromeda XVIII, is ~ 1.4 Mpc from the Galaxy (~ 600 kpc from M 31). Andromeda XIX, a satellite of M 31, is the most extended dwarf galaxy known in the Local Group, with a half-light radius of $r_h \sim 1.7$ kpc. This is approximately an order of magnitude larger than the typical half-light radius of many Milky Way dSphs (with M 31 dwarfs are generally more extended than their Milky Way counterparts). Andromeda XX, is one of the faintest galaxies discovered in the vicinity of M 31, with an absolute magnitude of order $M_V \sim -6.3$.

10.2 The Local Group as a laboratory

The LG provides us with a nearby laboratory, in fact, the nearest grouping of galaxies in which detailed studies can be done. Galaxies can be resolved allowing for example accurate and very deep colour-magnitude diagrams to be derived. As well,

some galaxies at the extremity of the LG may not have fallen into the group yet, whilst other galaxies orbital characteristics can be inferred. Low light level studies of such nearby galaxies allow us to determine where the stellar extent of the galaxies finish, and infer the extent of dark matter halos. One of the most interesting studies using the LG is to determine whether internal (star formation and feedback effects) or external factors (tidal stripping, ram pressure) are dominant in galaxy evolution. In the LG there is nearby gas not associated with our Galaxy. What is its origin? Studies of LG galaxies is a prime example of an evolving extension of 'near-field cosmology' (Freeman and Bland-Hawthorn 2002) that primarily concerns the Galaxy (and discussed further in Section 10.3).

10.2.1 Where do galaxies end?

Astronomers believe that large, massive dark matter halos exist around most if not all galaxies. For example, whilst the distance between the Galaxy and M 31 is ~ 700 kpc and if the luminous diameters of both galaxies are ~ 40 -50 kpc, a large fraction of the intervening distance could be taken up with their individual dark matter halos. The dark halos may even overlap. Since we can't directly detect dark halos, deep imaging to determine the optical light extent can provide an answer to "where do galaxies end"?

Deep exposure imaging (McConnachie *et al.* 2009), as seen in Figure 10.3, has shown stellar structure extending 150 kpc from M 31 and overlapping with stellar light extending 50 kpc from M 33. It is likely that stars exist between both galaxies and could exist as far away from parent galaxies as the virial radius of their dark matter halos (~ 300 kpc for M 31). Observations like this suggest that the extent of the stellar content of normal galaxies has been underestimated.

10.2.2 How do dwarf galaxies evolve?

Since the LG is dominated by dwarf galaxies, it seems natural to investigate the evolution of LG dwarfs. The results from such investigations may be global in nature, as it appears that LG dwarfs are similar to the dwarf galaxy population of the local universe (Weisz *et al.* 2011b). Dwarf galaxies are the predominant type of galaxy in the universe with number densities 10x and 50x greater than normal spirals and ellipticals respectively (Mo, van den Bosch and White, 2010). Within hierarchical structure formation models in Λ CDM cosmologies, they are the building blocks of larger galaxies.

Our Local Group (LG) has a large number of dwarf galaxies, some of which have orbital characteristics suggesting they either have not been, or are minimally, tidally disturbed by the larger galaxies (the Galaxy and M 31). These nearby dwarfs are the best galaxies in which the role of secular (internal, slow) processes in evolution

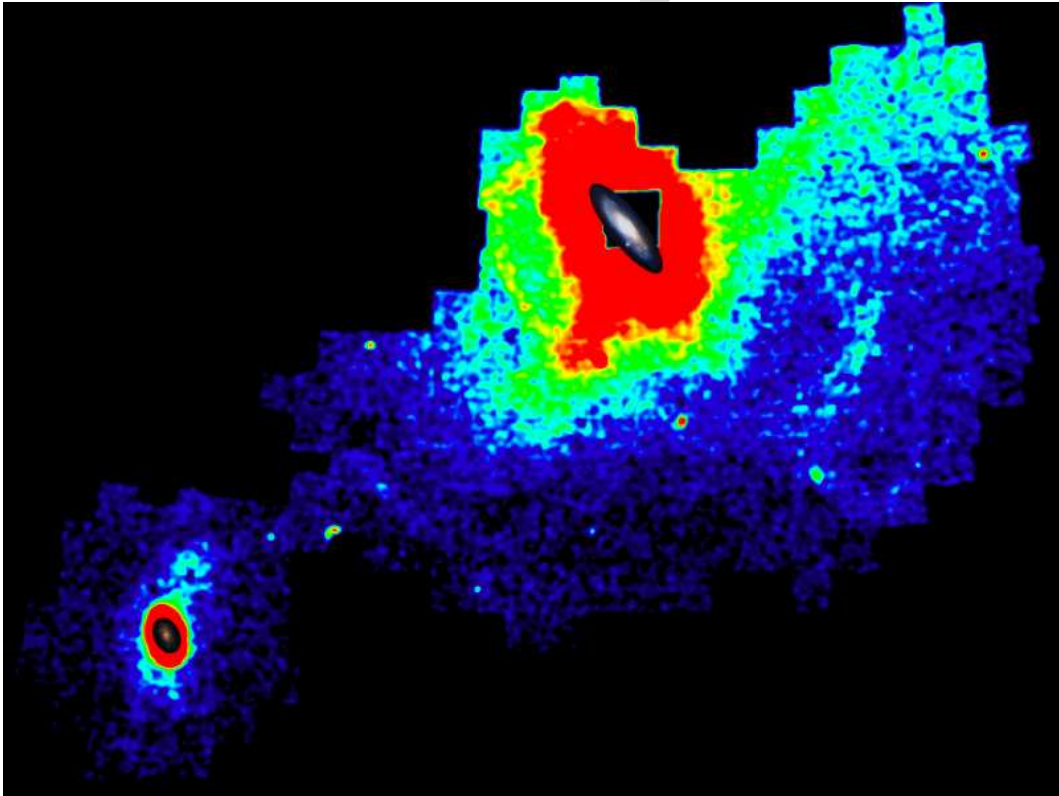


Figure 10.3: Stellar density map of the Andromeda-Triangulum region. A projection of the stellar density distribution with scale images of the disks of M 31 (top, right) and M 33 (bottom, left) overlaid. Credit: A. McConnachie. The small images of M 31 and M 33 courtesy T. A. Rector, B. A. Wolpa and M. Hanna (NRAO/AUI/NSF and NOAO/AURA/NSF). Reprinted by permission from Macmillan Publishers Ltd: Nature, vol. 461, p. 66., copyright (2009).

over long timescales can be explored.

The apparent morphology-density relation in the LG, (see Figure 10.4), in which gas-poor dwarf spheroidals (dSphs) are preferentially found closer to the Galaxy and M 31 than gas-rich dwarf irregulars (dIrrs) is often promoted as evidence of environmental processes (i.e. tidal and ram pressure stripping) influencing dwarf galaxy evolution. Do dIrrs evolve into dSphs in the vicinity of much larger, more massive galaxies, and if so, how does this occur? However there are exceptions to the relation (e.g. AndXII a dSph probably falling into the LG for the first time, Chapman *et al.* 2007) suggesting other processes can play important roles in low mass galaxy evolution. Additionally there is a third, and rarer class of dwarf, dTrans (Mateo 1998) with detectable gas, but little or no $H\alpha$, ionised hydrogen. These galaxies could be an evolutionary link between dIrrs and dSphs.

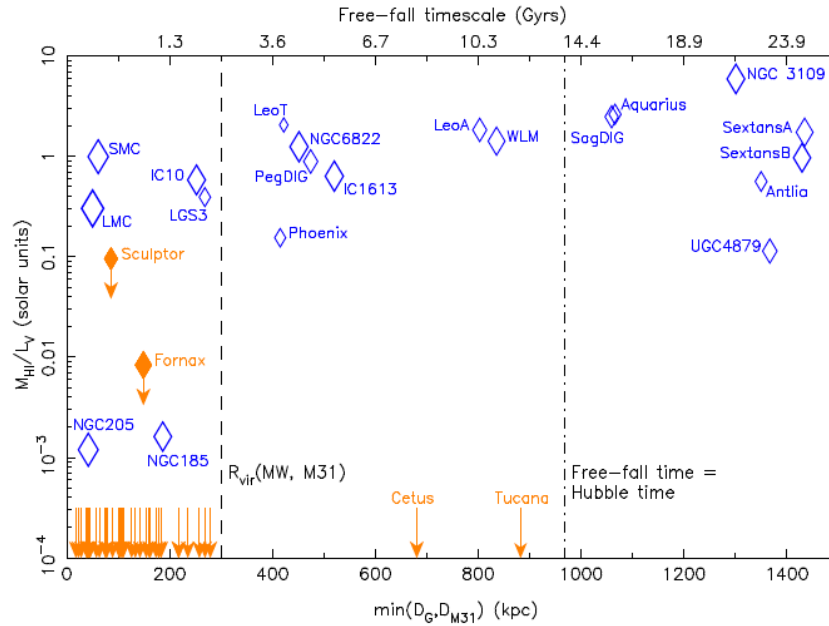


Figure 10.4: Luminosity normalised HI fraction versus proximity to the Galaxy or M 31 showing the LG morphology-density relation. Blue diamonds are galaxies with confirmed H I. Orange arrows show the separation of gas-deficient galaxies from either the Galaxy or M 31. Solid orange diamond symbols for Sculptor and Fornax indicate that a detection of H I is ambiguous. The vertical dashed line indicates the virial radius of the Galaxy/M 31. The top axis indicates the free-fall time in Gyrs to reach the Galaxy/M 31, and the dot-dash line near $\min(D_G, D_{M31}) = 1000$ kpc indicates where the free-fall time equals the Hubble time. From McConnachie 2012.

- A strong morphology-density relation exists in the LG, in which gas-poor dwarf spheroidals (dSphs) are preferentially found closer to the Galaxy/M 31 than gas-rich dwarf irregulars (dIrrs). This is often promoted as evidence of environmental processes (i.e. tidal and ram pressure stripping) due to the massive galaxies, the Galaxy and M 31 driving the evolutionary change between dwarf galaxy types.

Star Formation Histories (SFHs) describe the evolution of the baryonic content of galaxies. One of the best diagnostics of SFHs has come from deep HST imaging producing colour-magnitude diagrams (CMDs) detecting stars several magnitudes below the tip of the RGB (TRGB) and sometimes sampling the main sequence population. These show that whilst different rates of present day star formation (SF) occur in different classes of dSph, dTrans, dIrr (Tolstoy, Hill and Tosi 2009) all dwarfs possess old (>10 Gyr) stars.

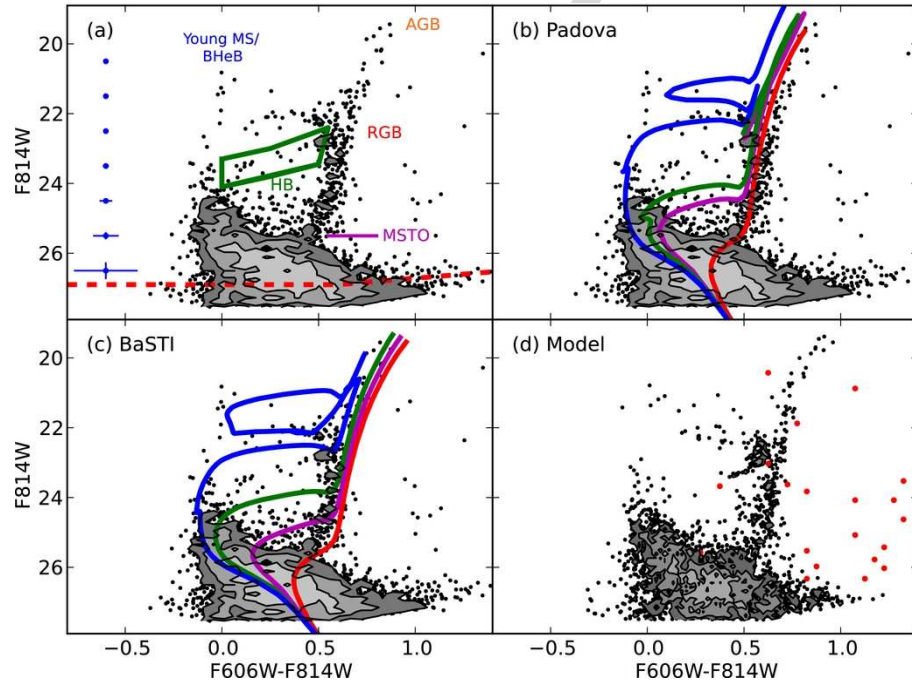


Figure 10.5: Deep HST/WFPC2 CMD of Leo T. (a) Several age sensitive features, including the horizontal branch (green box) and oldest MSTO (magenta) are shown. The red-dashed line represents the 50% completeness limit and blue error bars indicate photometric uncertainties. (b) The observed CMD of Leo T with Padova isochrones of 500 Myr (blue), 2 Gyr (green), 5 Gyr (magenta), and 10 Gyr (red) and a metallicity of $Z = 0.0005$. (c) Same as panel (b) only with the BaSTI isochrones, and a metallicity of $Z = 0.0003$. (d) A model CMD from the most likely SFH based on the Padova stellar libraries. The red points represent the intervening foreground stellar population. (from Weisz *et al.* 2012).

Figure 10.5 shows the HST CMD of the faint, $M_V = -8.0$ dIrr/dSph Leo T. Leo T is one of the faintest known star forming galaxies. The HST derived CMD extends ~ 2 mags. below the oldest (>10 Gyr) main sequence turn-off (MSTO) and allows the authors to determine that 50% of the total stellar mass of Leo T formed prior to $z \sim 1$ (~ 7.6 Gyr ago).

A major study of SFHs in 60 dwarfs (Weisz *et al.* 2011a) shows the typical dwarf has formed 60% of its stars by $z \sim 1$ regardless of its type. Figure 10.6 shows mean specific SFH (sSFH - the SFH normalised by the stellar mass of the galaxy) for dwarfs. Major differences in sSFH between dwarf types occur in the last 1 Gyr. Typical dSph, dIrr and dTrans formed $\sim 2\%$, 8% and 4% of their total mass respectively, and arguably dIrr have a rising sSFH, dTrans have flat sSFH and dSph a decreasing sSFH.

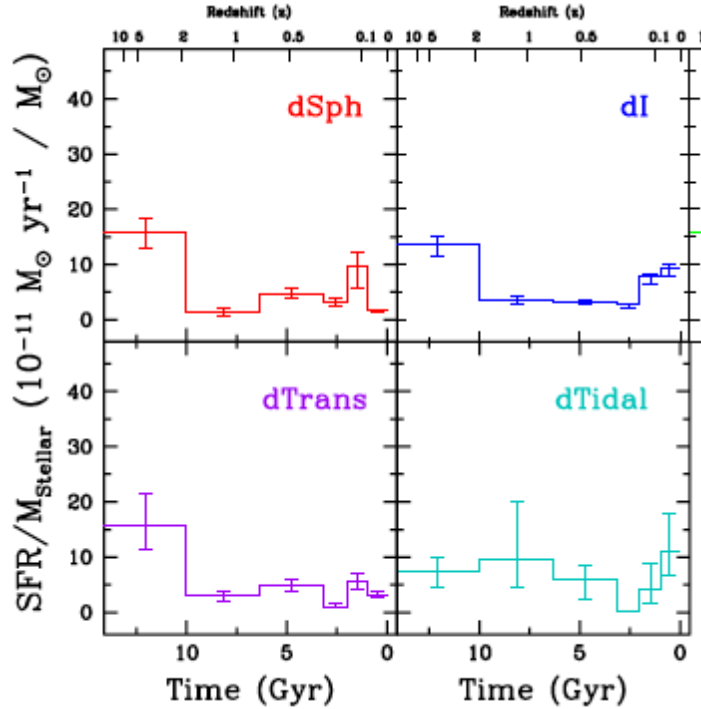


Figure 10.6: Mean specific SFH (sSFH) for dwarf types dSph, dIrr, dTrans and dTidal. dTidal are classified as condensing out of tidally disturbed gas in the M 81 group. (from Weisz *et al.* 2011a).

10.2.3 HVCs and the Magellanic Stream

High Velocity Clouds (HVCs) are clouds of interstellar gas that have substantially different velocities compared to what is expected due to the rotation of the gas disk of the Galaxy. It is thought that they are not associated with the Galaxy, and are probably infalling gas. HVCs are dominated by hydrogen, and have in general low metallicities. Their origin is currently debated, though it is likely they are either remnant gas left over from the formation of the Galaxy, or they are associated with other galaxies that have been tidally disturbed due to the influence of the Galaxy.

Figure 10.7 shows the distribution of HVCs colour coded by their velocity compared to the Local Standard of Rest, v_{LSR} in km s^{-1} . The Local Standard of Rest (LSR) (see Figure 10.8) is a reference used for radial velocities and is based on a position (R, Θ, z) in space moving in a circular orbit around the Galaxy centre, at the Sun's galactocentric distance. R is the galactocentric distance, Θ the azimuthal coordinate, and z is the distance above or below the plane of the Galaxy.

The velocity of the LSR, v_{LSR} is $\Pi_{LSR} = 0$, $\Theta_{LSR} = \Theta_0$, $Z_{LSR} = 0$ and remember it is not based on the orbit of the Sun since the Sun does not move in a circular orbit. Relative to the v_{LSR} the Sun has a velocity of 10 km s^{-1} towards the Galactic centre ($\Pi = -10 \text{ km s}^{-1}$), is travelling at 5 km s^{-1} faster in the direction of rotation

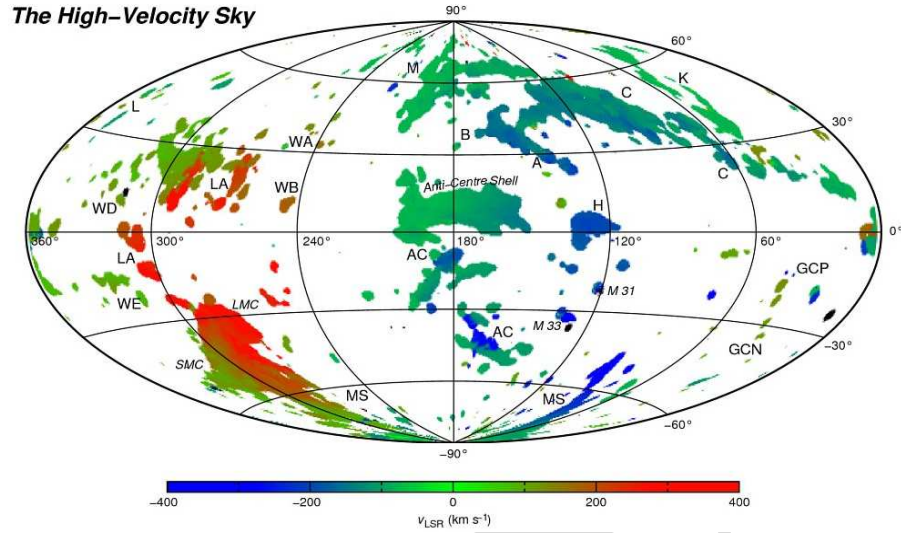


Figure 10.7: An all-sky map of high-velocity HI clouds. The map was generated from the Leiden/Argentine/Bonn (LAB) Galactic Survey (Kalberla et al. 2005) on the basis of a model of the HI gas distribution in the Milky Way. For each position in the sky a range of radial velocities for Galactic emission was derived for the Milky Way. All emission outside this velocity range was considered high-velocity gas and was integrated to create the map (in Galactic coordinates in Hammer-Aitoff projection above).

($\Theta = +5 \text{ km s}^{-1}$) and is travelling 7 km s^{-1} towards the north Galactic pole ($Z = +7 \text{ km s}^{-1}$). Hence the LSR reference frame accounts for the peculiar motion of the Sun of $\sim 16.5 \text{ km s}^{-1}$ with respect to the regular rotation of the Galaxy.

If we also want to correct also for the rotation of the Galaxy of 220 km s^{-1} the Galactic Standard of Rest (GSR) frame, can be derived from the LSR via

$$v_{GSR} = v_{LSR} + 220 \sin(\ell) \cos(b) \quad (10.6)$$

where ℓ and b are the Galactic longitude and latitude respectively. Whilst the IAU recommended values of rotation velocity $\Theta_0 = 220 \text{ km s}^{-1}$ and distance to the Galactic centre $R_0 = 8.5 \text{ kpc}$ are still routinely used, Brunthaler *et al.* (2011) suggest a revision is necessary. They have utilised VLBI observations to determine the proper motion of SgrA*, the radio source defining the centre of the Galaxy, to derive (a larger) $\Theta_0 = 239 \pm 7 \text{ km s}^{-1}$ and (a smaller) $R_0 = 8.3 \pm 0.23 \text{ kpc}$ than the standard IAU values.

HVCs are detected in a variety of sizes. Some span tens of degrees across the sky (i.e. features C, M, H in Figure 10.7), others are quite compact. Compact high velocity clouds (CHVCs) appear as condensed, usually asymmetrically shaped, many with bow-shock morphologies suggestive of ram pressure interactions with an ambient medium. Observations suggest they are $\sim 100 \text{ kpc}$ in distance, which sug-

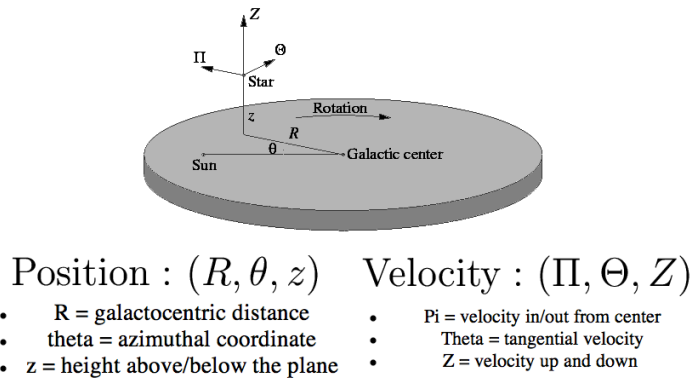


Figure 10.8: The LSR is a reference used for radial velocities and is based on a position (R, Θ, z) in space moving in a circular orbit with $\Pi_{LSR} = 0$, $\Theta_{LSR} = \Theta_0$, $Z_{LSR} = 0$ around the Galaxy centre, at the Sun's galactocentric distance.

gests they are not related to possible counterparts of primordial dark matter halos (distributed throughout the LG) predicted by Λ CDM structure formation models.

The Magellanic Stream is a filament of neutral (atomic) hydrogen, H I (Figure 10.9) first discovered in the early 1970s (Wannier and Wrixon 1972) covering $100^\circ \times 10^\circ$ of the sky. It lies within the Galactic halo and contains $\sim 2 \times 10^8 M_\odot$ of H I (Putman *et al.* 2003).

The H I system extends from the LMC to the SMC via a connecting bridge, then extends more than 70° across the sky. Putman *et al.* (1998) discovered a Leading Arm Feature (LAF) of gas moving in the opposite direction to the trailing feature of the Magellanic Stream. The most likely interpretation of the Magellanic Stream is that the LMC and SMC have passed close to, or through the halo of the Galaxy. Hydrogen gas has been gravitationally stripped out of the LMC and SMC and a stream is now attracted to the larger Galaxy.

A population of CHVCs (Figure 10.10) was detected (Westmeier and Koribalski 2008) in several filaments running parallel to the Magellanic Stream. The CHVCs may be associated with ionized gas filaments, and detections of O VI absorption in sight lines to distant quasars, at similar velocities to the CHVCs, are suggestive of associated extended, diffuse gas.

They have similar radial velocities, with a GSR $\sim -200 \text{ km s}^{-1}$ and a relatively small dispersion of 43.5 km s^{-1} suggestive of a common origin. The Magellanic Stream may be much wider (and more complex) than originally thought.

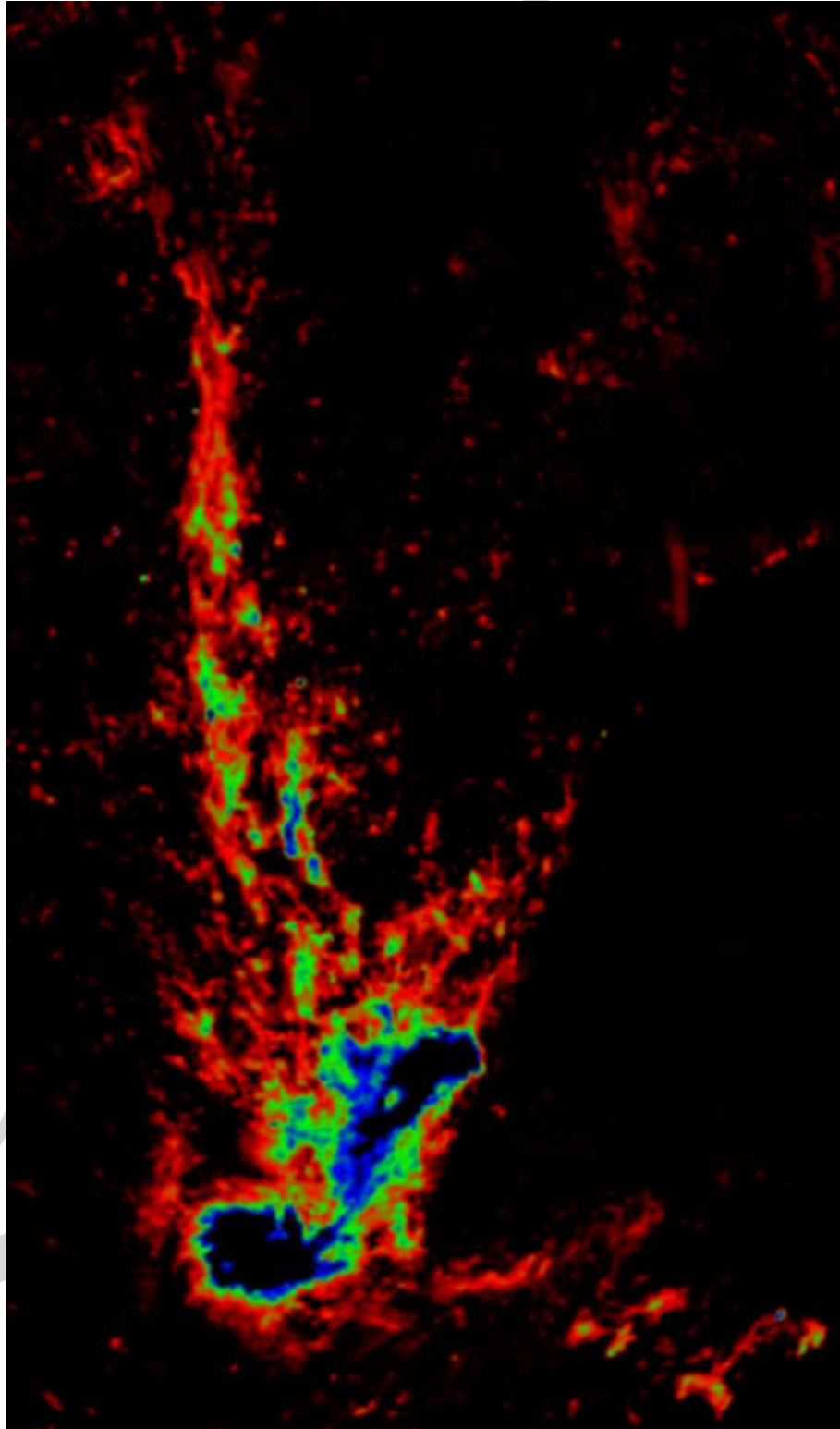


Figure 10.9: The radio H I Magellanic Stream starts at the bottom of the image where the large condensations indicate the positions of the LMC (left) and SMC (right) at Declination $\sim -70^\circ$ and extends upwards to Declination $+02^\circ$. The image contains H I at velocities between -400 and $+400$ km s $^{-1}$. Credit: M. Putman.

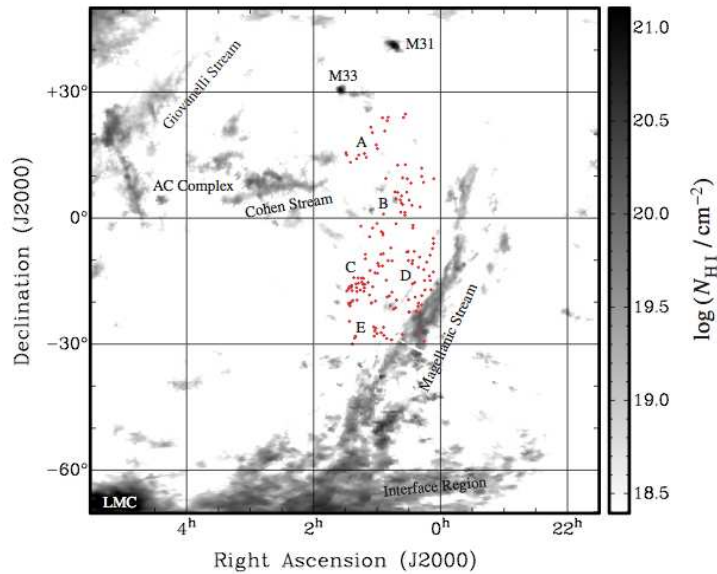


Figure 10.10: Positions of Compact HVCs labelled A to E (red dots) that are distributed almost parallel to the Magellanic Stream. The LMC is at bottom, left, and M 31 and M 33 are top, middle. Credit: Westmeier and Koribalski (2008).

- High Velocity Clouds (HVCs) are clouds of interstellar gas that are not associated with the Galaxy, and are probably infalling gas. Their origin is currently debated, though it is likely they are either remnant gas left over from the formation of the Galaxy, or they are associated with other galaxies that have been tidally disturbed due to the influence of the Galaxy.

10.3 The Galaxy

Let us now venture further into the Local Group laboratory, and look more closely at the nearby environment, our Galaxy. Whilst we are located inside the Galaxy, and our viewpoint is somewhat restricted, observations of our Galaxy provides the most detailed picture of the stellar and gaseous properties of a mid-mass range, $\sim 10^{12} M_{\odot}$ spiral galaxy.

10.3.1 Chemical, dynamical and structural components

Chemical components: Chemically distinct stellar populations typically display related structural and dynamical properties. Combined, this information allows astronomers to piece together the formation and evolution histories of each population.

The chemical 'tags' include abundances of such elements as Mg, Si, O, Ca and Fe.

The 'metallicity' of a star or population of stars is related to the amount of heavy elements (not including hydrogen or helium) it has. The metallicity is usually denoted by the iron abundance $[Fe/H]$ and we have defined it in Section 5.1. The metallicity distribution of halo stars is approximately

$$-3 < [Fe/H] < -1 \quad (10.7)$$

with a peak at $[Fe/H] \sim -1.5$. In comparison the thin disk has

$$-0.5 < [Fe/H] < 0.3 \quad (10.8)$$

The thick disk has

$$-2.2 < [Fe/H] < -0.5. \quad (10.9)$$

and the Galactic bulge has

$$-1 < [Fe/H] < 0.5 \quad (10.10)$$

Dynamical components: Observations that allow the measurement of individual velocities of stars are very powerful, but even the velocity derived by integrated starlight along a line-of-sight can prove informative. Stellar populations in which individual velocities can be measured allow an integrated dynamical picture to be made from a sample of stars and the dispersion, or σ , of velocities can provide an important energetic diagnostic. Velocities of distant, unresolved stars along a line of sight are also described by their dispersion, or σ , as measured by the integrated Doppler broadening of spectral lines. Higher σ indicates larger broadening of stellar lines, thus a wider distribution of stellar velocities.

Large σ populations are thus more energetic and are regarded as 'hotter' dynamical systems - likewise lower σ populations indicate 'colder' systems. Dynamically hot stellar systems such as spiral galaxy bulges or halos are kinematically dominated by the random motions of stars, with their σ the same magnitude as the rotation speed. Spiral disks which have rotation speeds at least a few times larger than σ are regarded as dynamically cold systems.

Structural components: The Galaxy (see Figure 10.11) has an extended, old stellar halo with a diameter ≥ 100 kpc, in which ~ 150 metal-poor globular clusters reside. The halo has a $\sigma \sim 120$ km/s and no net rotation (but see Section 10.4.1), and is thus supported almost completely by random motions of stars.

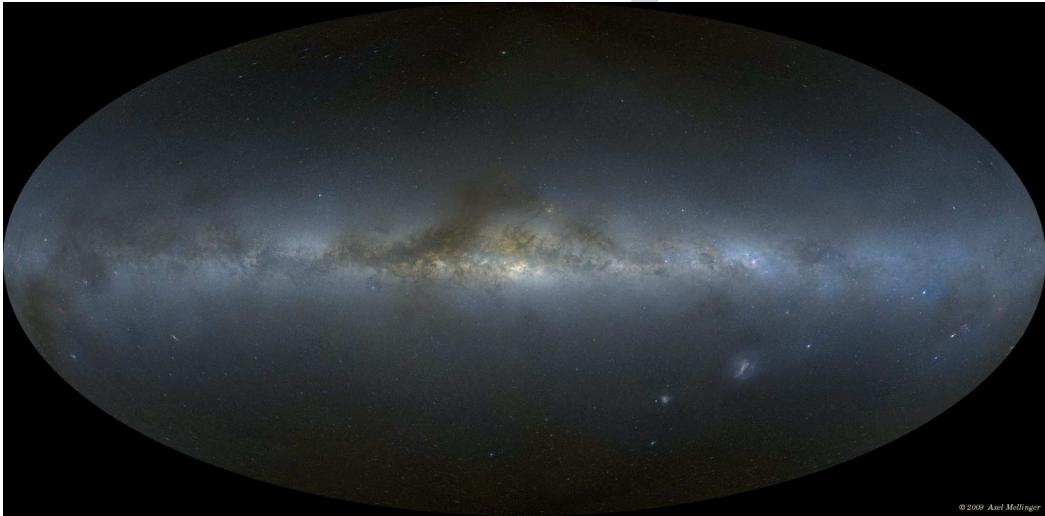


Figure 10.11: A colour all-sky panorama image, in Hammer-Aitoff projection, of the Galaxy. Credit: Axel Mellinger, Mellinger (2009).

We recommend a visit to

<http://galaxy.phy.cmich.edu/~axel/mwpan2/krpano/>

to view see a zoomable Flash-based panorama of Figure 10.11.

A Galactic bulge exists. It has a diameter of ~ 2 kpc, comprising mainly old stars, centred on the Galactic nucleus and has $\sigma \sim 100$ km/s.

The Galaxy has a disk that has two distinct components. A thin disk of diameter of ~ 50 kpc, with a vertical scale height¹ of 300 pc, and a $\sigma \sim 10$ km/s. A fainter, thick disk has a scale height some three times larger than the thin disk, of ~ 1 kpc, and a hotter dispersion of $\sigma \sim 40$ km/s. Similar thick disks have been observed in other galaxies suggesting they may be quite ubiquitous in disk galaxies. Thick disks can be created by mergers of smaller (dwarf) galaxies. At the position of the Sun, about 8.3 kpc from the Galactic centre, the disk rotation speed is ~ 220 km/s.

Astronomers believe that the Galaxy has a central stellar bar and is a loosely wound, barred spiral galaxy of Hubble type SBbc (Sandage 1975) or de Vaucouleurs revised Hubble-Sandage type SAB(rs)bc (de Vaucouleurs and Pence 1978).

In addition to its visible structure, and similarly to other spiral galaxies, the Galaxy contains a halo of dark (most likely non-baryonic) matter. This dark halo extends well beyond the edge of the disk, and the motions of galaxies around the Galaxy suggest it has a total mass of several times $10^{12} M_{\odot}$ (see Section 10.1.2)

¹Scale height is a distance measure over which a quantity decreases by the factor e, the base of natural logarithms.

which is about ten times the mass of visible material.

10.3.2 Oldest elements

Nucleo-cosmochronology provides a way to age-date individual metal-poor stars in our Galaxy, and thus provide constraints on the oldest Galactic building blocks. Abundances of neutron-capture elements associated with the r-process such as Europium (atomic symbol Eu), Osmium (Os), and Iridium (Ir) as well as the radioactive elements Thorium (Th) (^{232}Th , half-life of $\tau_{1/2} = 14.0$ Gyr) and Uranium (U) (^{238}U , $\tau_{1/2} = 4.5$ Gyr and ^{235}U , $\tau_{1/2} = 0.7$ Gyr) allow age estimates to be made. Galactic stars with $[\text{Fe}/\text{H}] < -5.0$ (or extreme Population II) are now being discovered and are called hyper-metal-poor (HMP).

Definition: Neutron capture and the r-process

Korn *et al.* (2009) find that the HMP star HE 1327-2326 with $[\text{Fe}/\text{H}] \sim -5.6$ is 13 Gyr old. A non-detection of a Li resonance line is at odds with the WMAP based primordial lithium abundance, however it is quite possible that unknown mechanisms alter the surface composition of such old HMP stars and that current modelling techniques need improving. Based on the abundances of Eu, Os, Ir, Th and U the metal-poor star HE 1523-0901 with $[\text{Fe}/\text{H}] = -3.0$ has an averaged stellar age of ~ 13 Gyr (Frebel *et al.* 2007). Whilst the age errors of these metal-poor stars are between 2-5 Gyr for individual chronometers, it is inferred that many of the HMP stars are representative of the stellar content of the 1st Gyr of the Galaxy.

10.4 Formation and evolution of the Galaxy

Through a combination of observations, theory and computer simulations the Star Formation History (SFH) of the main components of the Galaxy, can be deduced. This information combined with the structural and dynamical information described above in Section 10.3.1, can be used to draw significant conclusions about the formation and evolution of the Galaxy (Freeman and Bland-Hawthorn 2002; Wyse 2009). The following will summarise the knowledge about the main Galactic components, halo, bulge, thin and thick disk in relation to predictions of the Λ CDM Concordance model (Section 2.10).

10.4.1 Halo

The halo contains about 1% of the total Galactic stellar mass. It is the oldest structural component of the Galaxy and is metal-poor with stellar properties that

are indicative of short-duration star formation with enhanced elemental abundances reflecting rapid chemical enrichment via type II SNe.

Definition: Type Ia, II SNe

At least part of the halo was built by the accretion of smaller, metal-poor galaxies. Populations from these galaxies display larger stellar age ranges and prolonged chemical enrichment with contributions from Type Ia SNe leading to more enhanced Fe enrichment. Some old, metal-poor satellite galaxies could however assimilate into the field halo without detection. Satellite accretion would heat up the disk, but the Galaxy has a dominant thin disk. Therefore the bulk, $\sim 90\%$ of the halo was most likely built prior to the creation of the thick disk, and hence at least 8 Gyr ago and probably closer to 12 Gyr ago.

Recently evidence has been presented (Carollo *et al.* 2010; Beers *et al.* 2012) based on Sloan Digital Sky Survey data that the halo can be resolved into two distinct (inner and outer) components in which the outer component displays a net retrograde rotation signature and higher velocity dispersion than the inner halo. Other evidence, both observational and based on simulations also suggest that dual component halos may be a generic feature of large disk galaxies. An *et al.* (2012) suggest a two component halo with peaks at $[\text{Fe}/\text{H}] \approx -1.7$ and -2.3 is also a good representation, with the more metal-poor component comprising 20-35% of the halo in the range of heliocentric distances 5-8 kpc.

10.4.2 Evidence of satellite accretion in the halo

Whilst the bulk of the halo probably formed from accreted satellites at $z > 2$ there is also evidence of ongoing accretion. For example, the Sagittarius dSph galaxy was discovered (Ibata, Gilmore and Irwin 1994), ~ 24 kpc distant, to be on track to plunge through the disk of the Galaxy, after probably already doing this several times, every 100-200 million years. It appears to be on a polar orbit and is in the process of being tidally disrupted.

The "Spaghetti project" (e.g. Morrison *et al.* 2000; Harding *et al.* 2001) searched for kinematic substructure in the halo to answer the question: how much of the Galaxy's halo was accreted from dwarf galaxies like the Sgr dSph? Simulations presented by Harding *et al.* (2001), see Figure 10.12, suggest that satellite infall could produce many substructure signatures that can be relatively easily detected by 'chemical tagging' (see Freeman and Bland-Hawthorn 2002 and Section 10.3.1).

Dohm-Palmer *et al.* (2001) detect giant stars in numbers greater than expected for a smooth halo model. Radial velocities of these giant stars agree with predictions

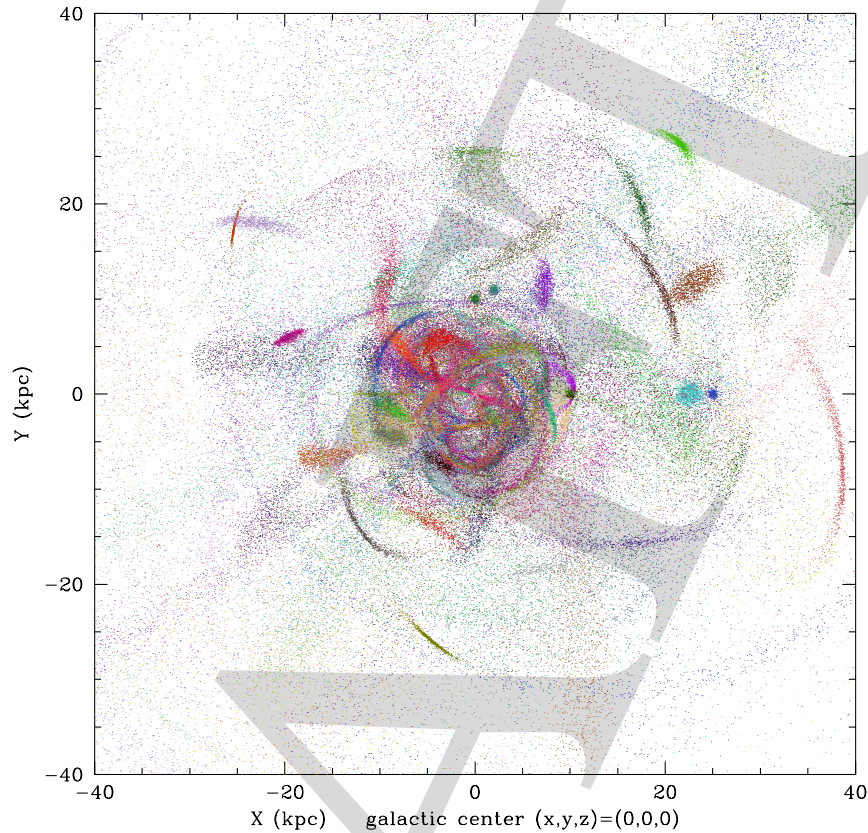


Figure 10.12: A simulation of what a halo might look like as formed by 50 dwarf galaxy accretion events during the last 10 Gyr. This can be viewed at <http://astronomy.case.edu/heather/spag.html> Credit: Paul Harding, Heather Morrison.

of the dynamical evolution of the Sgr dSph tidal debris. Ibata *et al.* (2001) find that carbon stars associated with the Sgr dSph tidal debris suggest a similar age of the debris to the halo substructure age implied by SDSS data. Belokurov *et al.* (2006) used the SDSS to study the leading arm structure of the Sgr stream as well as other tidal stream stellar structures (see Figure 10.13) in the Northern Galactic Cap region.

Approximately 10% of the mass of the Galaxy halo is associated with tidal debris from the Sgr dSph and smaller Hercules-Aquila cloud at Galactocentric distances between 15 and 60 kpc. Law and Majewski (2010) introduce a triaxial dark matter halo model in the shape of a nearly oblate ellipsoid to describe the position, distance and radial velocity of the Sgr dSph tidal streams. Using such a model the leading and trailing tidal arms are well described, but the low surface brightness 'bifurcation' that parallels the leading arm is not. They estimate $M_{SgrdSph} = 2.5^{+1.3}_{-1.0} \times 10^8 M_{\odot}$ and that Sgr dSph has been orbiting the Galaxy for > 3 Gyr. The introduction

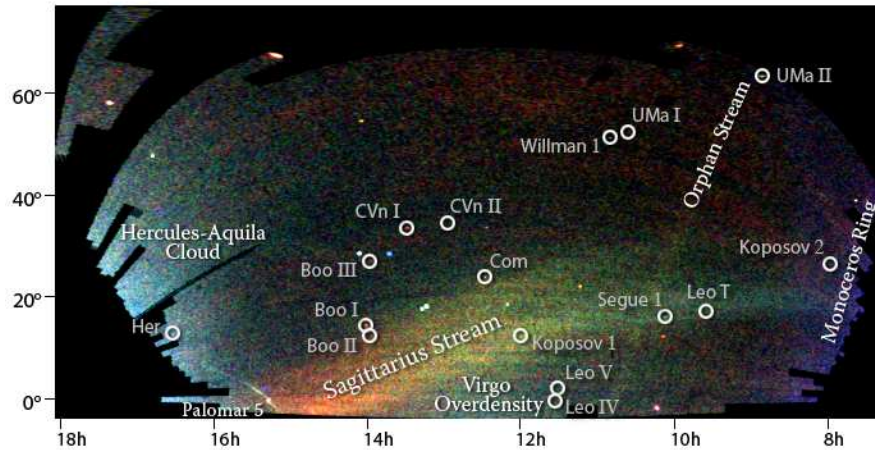


Figure 10.13: The 'Field of Streams' distribution of main sequence turnoff stars imaged by SDSS. Stars are colour coded with $20.0 < r \leq 20.66$ (blue, the nearest stars), $20.66 < r \leq 21.33$ (green) and $21.33 < r \leq 22.0$ (red, the most distant stars). The streams (Sagittarius, Orphan and Monoceros) are tidally induced debris remnants of dwarf galaxies. Circles indicate positions of dwarf galaxies and star clusters. The disputed globular cluster Palomar 5 is also indicated. Credit: V. Belokurov, see Belokurov *et al.* (2006).

of a non-axisymmetric component to the Galactic gravitational potential (via such a triaxial dark matter halo model) is noted not to be strongly aligned with the current CDM paradigm, and may mimic some unknown additional component such as the gravitational influence of the Magellanic Clouds.

- Despite containing 1% of the total Galaxy mass, the halo has provided clues to the earliest processes of formation. The halo forms from accreted satellite galaxies at ages > 10 Gyr ($z \sim 2$). The halo may not be homogeneous as recent observations suggest two distinct (inner, outer) components in which the outer component displays a net retrograde rotation signature and high velocity dispersion.

10.4.3 Bulge

The bulge is dominated by old, 10-12 Gyr stars as shown by the existence of RR Lyrae populations. As well, red giants in the bulge have metallicities closer to old, disk stars rather than very old, metal-poor halo stars. Though some younger stellar populations have been observed close to the bulge center near the disk plane. Mergers can build the bulge population via instabilities in the disk, and satellite core

regions may survive and also build the bulge. The bulge of the Galaxy may have an elongated or boxy shape which may also suggest partial creation by instabilities in the disk. The dominant old population of the bulge suggests that the major epoch of construction was a narrow, ~ 1 Gyr age range at $z > 2$. It is therefore possible that the bulge and the thick disk (see Section 10.4.5) formed concurrently. The Galactic bulge has a metallicity range of $-1 < [\text{Fe}/\text{H}] < 0.5$.

10.4.4 Thin disk

The ages of the oldest disk stars range between 10 and 12 Gyr, with a typical average age of a disk star cited around 9 Gyr. Hipparcos data suggests star formation in quasi-periodic bursts every ~ 0.5 Gyr over the last 3 Gyr. This may be suggestive of spiral arm passages prompting periodic star formation. Other studies have extended the lookback time and derive a broad maxima of star formation between 3-5 Gyr ago (and similar to the global SFH shown in Section 7.2). The Galaxy, pleasingly, appears typical. The thin disk has $-0.5 < [\text{Fe}/\text{H}] < 0.3$.

Of course accurately determining the star formation history of the local population thin disk from nearby stellar samples is fraught with problems. Old stars in the local disk could well have formed elsewhere. Radial mixing can explain the detection of metal-poor disk stars as they may have originated in the outer disk.

Lee *et al.* (2011) use $[\alpha/\text{Fe}]^2$ ratios to separate thin and thick disk samples of G dwarf stars in the SDSS Sloan Extension for Galactic Understanding and Exploration (SEGUE) survey. The eccentricities and dynamical properties of the two samples suggest that radial migration has influenced the thin disk, but not the thick disk. Mergers of satellites may also inject a range of stars into near-circular orbits in the solar neighbourhood.

10.4.5 Thick disk

The thick disk was discovered by Gilmore and Reid (1983). The thick disk is 10-20% as massive as the thin disk and the bulk of thick disk stars are old, between 10-12 Gyr. With its larger scale height than the thin disk, the more energetic thick disk is believed to have formed by accretion events or minor mergers. The old age of thick disk stars, ≥ 10 Gyr, suggest the last significant minor merger took place at $z \geq 2$. The thick disk has $-2.2 \leq [\text{Fe}/\text{H}] \leq -0.5$.

Figure 14 in Edvardsson *et al.* (1993) that plots age and metallicity for 189 nearby field F and G disk dwarfs can be used to characterise a relatively clear subdivision

²The α refers to 'alpha elements' (some even-Z elements) that are overabundant relative to iron at low metallicity. $[\alpha/\text{Fe}]$ is usually denoted as the average of $[\text{Mg}/\text{Fe}]$, $[\text{Si}/\text{Fe}]$, $[\text{Ca}/\text{Fe}]$ and $[\text{Ti}/\text{Fe}]$.

between thin and thick disk stars in the Galaxy. In this study thick disk stars have $[\text{Fe}/\text{H}] < -0.4$ and ages greater than 10 Gyr. Table 10.4.5 summarises the velocities of both disk populations, and we can see that the velocity dispersion (in radial, R ; tangential, ϕ ; and out of the plane, z directions) of the thick disk is twice that of the thin disk.

Thick disks seem inevitable in Λ CDM cosmological models due to late merging of satellites and subsequent heating of existing thin disks. However as Wyse (2009) points out, constraining the last minor merger in the Galaxy to $z \geq 2$ (10 Gyr ago) is very atypical, as minor mergers should continue well past this redshift/age limit. In fact we do detect ongoing minor mergers (e.g. Sgr dwarf; Ibata, Gilmore and Irwin 1994) and these have to have small effects on the current old, thick disk.

Characteristic velocities of the thin and thick disks

	$\langle v_\phi \rangle$	σ_R	σ_ϕ	σ_z
Thin disk	-6	34	21	18
Thick disk	-36	61	58	39

Notes

- As shown in Binney and Merrifield (1998) with data from Edvardsson *et al.* (1993)

- The Galaxy disk has two distinct components. A thin disk of diameter of ~ 50 kpc, with a vertical scale height of 300 pc, and $\sigma \sim 10$ km/s. A fainter, thick disk has a scale height some three times larger than the thin disk, of ~ 1 kpc, and a hotter dispersion of $\sigma \sim 40$ km/s.

10.4.6 Working model of formation of the Galaxy

It is regarded as a cliché to continually use the term 'golden-age' to describe a period of rapid advancement in an area of research. However the current advances in determining the chemical, structural and kinematical properties of individual stars via multiplexing spectroscopic surveys such as SDSS/SEGUE, RAdial Velocity Experiment (RAVE) and others to advance our understanding of the formation and evolution of the Galaxy, would certainly be an exception to the rule. The power of multiplexing surveys comes from the ability to identify the long-lived chemical and kinematic phase-space signatures of merger population progenitors.

Under the Λ CDM paradigm formation of structure is hierarchically driven, with larger objects being built by the mergers of smaller objects. The building blocks will be dark matter halos with baryonic matter, and the result will be dependent on mass ratios, relative densities and the relative fractions of dissipationless (dark matter, stars) and dissipational (gas) material. In this formation model the halo, thick disk and part of the thin disk will be formed via early merger processes. The bulge may have formed later (or over a prolonged period) from processes in the thin disk.

The halo forms from accreted satellite galaxies at ages > 10 Gyr ($z \sim 2$). Section 10.4.1 mentions recent results suggesting that the halo should not be regarded as homogeneous. The first globular clusters are formed, as well as the beginning of the central black hole. Some of the globular clusters may be remnants of accreted satellite galaxies.

Metallicity enhancement was rapid due to peak star formation activity, as stars in the core regions reached $[\text{Fe}/\text{H}] \sim -1$. Freeman and Bland-Hawthorn (2002) note that the fraction of Fe produced by SN II events can constrain the number of supernova occurrences a given parcel of gas has experienced. In a closed system a few SN II events give $[\text{Fe}/\text{H}] \approx -3$, 30-100 events give $[\text{Fe}/\text{H}] \approx -1.5$ and possibly a thousand events give $[\text{Fe}/\text{H}] \approx [\text{Fe}/\text{H}]_{\odot}$. These numbers are approximate, and also need to consider the increasing contribution of SN Ia events to Fe as populations age.

The majority of baryons settle into the total disk, with 10% of them in the thick disk. Thin disks are easily destroyed by mergers, hence our thin disk formed predominantly after $z \sim 1$ and constrains major mergers from occurring after $z \sim 1.7-2$ (Wyse 2009, 2010). The old mean ages of stars in the bulge and thick disk suggest that any mergers after $z \sim 2$ would be predominantly low density, gas-rich systems. Minor mergers can “puff up” a pre-existing thin disk into a thick disk.

The bulge grows by the addition of thin disk stars during minor mergers. Torques due to mergers can force gas into the centre, contributing to the bulge stellar population.

It is worth remembering that the error in absolute stellar ages is at best 2 Gyr, which is roughly the age difference between $z = 2$ and $z = 5$. In summary a rapid mass assembly, and quiescent merging history (since $z \sim 2$, 10 Gyr ago) most likely explains the current observed properties of the Galaxy, though whilst this is unusual in Λ CDM models, analogues (extended disks with chemical enrichment) do exist at $z \sim 2$.

10.4.7 Missing satellites in the framework of CDM cosmologies

Whilst the Λ CDM structure formation model does match many key observational constraints, there is a specific mismatch with relation to the Galaxy. N-body simulations always predict an overabundance of dark subhalos within dark halos, which is not consistent with the number of satellites orbiting the Galaxy (Frenk and White 2012). It is sometimes called the 'satellite problem'. The answer to this conundrum may be related to the way low mass galaxies form and evolve. It is likely that early reionisation energises gas and prevents condensation, and that supernovae and hot, young stars may inhibit the formation of successive stellar generations (Kauffmann, White and Guiderdoni 1993).

Boylan-Kolchin *et al.* (2010) utilise the Millennium-II Simulation (MS-II) to do a statistical study of Milky Way-mass halos. One important discussion is whether the Galaxy halo is typical of others of similar mass. In other words is the Milky Way a typical galaxy for its halo mass? The authors assume a halo mass of $1 \leq M_{vir,MW} \leq 3 \times 10^{12} M_{\odot}$ (see also Section 10.1.2) which has a factor of 3 uncertainty. The existence of the LMC and the SMC are useful constraints, and the probability of hosting a subhalo capable of containing the LMC, or having two subhalos with the LMC and SMC are found to be 3-8% for $M_{vir,MW} = 1 \times 10^{12} M_{\odot}$ but markedly jump to 20-27% for $M_{vir,MW} = 2.5 \times 10^{12} M_{\odot}$. However to increase the hosting probability of known galaxies like the LMC and SMC the heavier halo mass required places similar restrictive timescale constraints on the merger history (i.e. a quiescent merger history since $z \sim 2$ - see Section 10.4.6) which has implications for the thin disk.

- Under the Λ CDM paradigm formation of structure is hierarchically driven, with larger objects being built by the mergers of smaller objects. The building blocks will be dark matter halos with baryonic matter. A rapid mass assembly, and quiescent merging history (since $z \sim 2$, 10 Gyr ago) most likely explains the current observed properties of the Galaxy, though this is unusual in Λ CDM models.

10.5 The future of the Local Group

The members of the LG are now interacting due to their mutual gravitational attraction, and are not moving away from each other according to the general expansion of the universe. A number of galaxies are most likely falling into the LG for the first time. The timescale for such galaxies to fall from rest under the influence of gravity and encounter either the Galaxy or M 31 is the "free-fall" time, t_{ff} , and is given by

$$t_{ff} \simeq 14.4 \text{ Gyr} \left(\frac{r}{1 \text{ Mpc}} \right)^{\frac{3}{2}} \left(\frac{M}{10^{12} M_{\odot}} \right)^{-\frac{1}{2}} \quad (10.11)$$

McConnachie (2012) lists Sagittarius dIrr, Aquarius dIrr/dSph, NGC 3109, Sextans A, Sextans B, Antlia and UGC 4879 (dIrr/dSph) as having $t_{ff} > t_0$, the Hubble time (refer to equation 1.13). Hence for these galaxies that are between 1.0 and 1.5 Mpc distant from the centre of the LG, it is a reasonable assumption that their evolution has not been influenced by either of the two large, dominant galaxies of the LG.

van der Marel *et al.* (2012b) have used the transverse velocity of M 31 (van der Marel *et al.* 2012a - see Section 10.1.2) to determine that the Galaxy and M 31 will merge in 5.9 Gyr, after a first pericenter passage 3.9 Gyr from now, to ultimately resemble an elliptical galaxy. The lack of nearby large galaxies to the Galaxy and M 31 suggests their orbit does not contain significant angular momentum, implying that the merger process will be predominantly head-on.

The authors of van der Marel *et al.* (2012b) and NASA, ESA and F. Summers (STScI) provide some informative video visualizations of the merger process at

<http://hubblesite.org/newscenter/archive/releases/2012/20/video/j/> and

http://www-int.stsci.edu/~marel/M31/M31_PaperIII_fig16c.mp4 (a 99 MB mp4 file).

- The Galaxy and M 31 will merge in 5.9 Gyr, after a first pericenter passage 3.9 Gyr from now, to ultimately resemble an elliptical galaxy.

Let's now consider the LG with respect to its surroundings. Of somewhat troubling importance is the seemingly large derived motion of the LG with respect to the CMB. Scott and Smoot (2004) find that

$$v_{LG} = 627 \pm 22 \text{ km s}^{-1} \quad (10.12)$$

toward $(\ell, b) = (276^{\circ} \pm 3^{\circ}, 30^{\circ} \pm 3^{\circ})$. Kocevski and Ebeling (2006) use an X-ray selected galaxy cluster sample to determine that 44% of the LG motion is due to infall into the region of the Great Attractor, an overdensity of galaxies ~ 80 Mpc distant in the Centaurus direction, near to Abell 3627, that harbours $\sim 10^{15} M_{\odot}$. The remaining amount of motion is due to more distant overdensities between 130 and 180 h^{-1} Mpc, primarily the Shapley supercluster, and contributions from the

Horologium-Reticulum supercluster, and Abell 3667 and Abell 3391 clusters.

- The LG has a velocity of $v_{LG} = 627 \pm 22 \text{ km s}^{-1}$ with respect to the CMB. About 44% of the LG motion is due to the infall into the region of the Great Attractor, and the remaining amount of motion is due to more distant overdensities between 130 and 180 h^{-1} Mpc, primarily the Shapley supercluster.

The collective properties of globular clusters in the Local Group have been studied in order to understand the resultant galaxy merger that will eventually occur. Under the assumption of a dissipationless merger (beginning in 3.9 Gyr according to van der Marel *et al.* 2012b), primarily of the Galaxy and M 31 but including satellites and associated neighbours, Forbes *et al.* (2000) speculate that the resultant elliptical galaxy will have $M_V \sim -21$ and possess 700 ± 125 globular clusters, assuming no creation or destruction of globulars.

The long-term future of the LG is ultimately tied to the future behaviour of the universe. We shall discuss a number of related issues in the Chapter 11. In the short term (the next ~ 5 Gyr) the LG will continue to move towards the Virgo cluster and at the same time the Galaxy and M 31 will merge. Not long after these events the accelerated expansion of the universe will constrain all subsequent motion. The LG will never reach the Virgo cluster and distant objects will eventually (~ 150 Gyr from now) disappear past our observable horizon. Our view of the universe will then consist (only) of our MW-M 31 merger galaxy in which we reside. Looking onwards to extreme times ($> 10^{14}$ years) we shall witness the long-term decay (see Section 11.2) of the constituents of our Galaxy.

- The LG will continue towards the Virgo cluster, but never reach it. In the far future the LG will be isolated due to the accelerated expansion of the universe.

10.6 Case study: Strangers in the Night: Discovery of a Dwarf Spheroidal Galaxy on its First Local Group Infall

Case study: Strangers in the Night: Discovery of a Dwarf Spheroidal Galaxy on its First Local Group Infall

Chapman, S.C. *et al.* (2007) *Ap.J.*, **662**, L79.

A PDF copy of paper can be viewed from this link:
http://iopscience.iop.org/1538-4357/662/2/L79/pdf/1538-4357_662_2_L79.pdf

Summary:

Keck Observatory observations show the And XII dwarf spheroidal galaxy to be moving rapidly through the Local Group and falling into the Local Group from ~ 115 kpc beyond M 31. And XII is therefore falling into a dense galactic environment for the first time.

Review questions:

1. Explain how the velocity of the dwarf galaxy was obtained, and why only 8 stars were associated with And XII out of 49 stars observed?
2. Apart from the observed Keck Observatory velocities how was galaxy membership (and distance) determined?
3. Comment on the upper limit detection of H I ($< 3 \times 10^3 M_{\odot}$) with respect to its present epoch position.

10.7 Case study: The Dawning of the Stream of Aquarius in RAVE

Case study: The Dawning of the Stream of Aquarius in RAVE

Williams, M.E.K. *et al.* (2011) *Ap.J.*, **728**, 102.

A PDF copy of paper can be viewed from this link:
http://iopscience.iop.org/0004-637X/728/2/102/pdf/apj-728_2_102.pdf

Summary:

Using data from the RAdial Velocity Experiment (RAVE) 15 stars are identified as belonging to a dynamically distinct, and previously unknown substructure in the halo of the Galaxy.

Review questions:

1. Explain how significant the stream is when compared to the the velocity expected for the thick disk and halo at the line-of-sight of the observation (ℓ , b) = $(55^\circ, -60^\circ)$.
2. Despite the lack of an overdensity of stars near the streams velocity range, and the large distance range (0.4 to 9.4 kpc) inferred, discuss how the authors decided upon the progenitor being a single, distinct object.
3. The authors performed some simple dynamical simulations of a satellite galaxy being disrupted by the gravitational field of the Galaxy. Describe the results, including the choice of the two starting timescales used (-700 Myr and -5 Gyr), and the conclusions based on phase-mixing arguments.

10.8 Key Concepts

Key concepts

- Our Galaxy resides in the Local Group which contains at least 70 galaxies. The Galaxy and the Andromeda galaxy M 31 dominate the Local Group, which has overcome the general expansion of the universe.
- A strong morphology-density relation exists in the LG, in which gas-poor dwarf spheroidals (dSphs) are preferentially found closer to the Galaxy/M 31 than gas-rich dwarf irregulars (dIrrs). This is often promoted as evidence of environmental processes (i.e. tidal and ram pressure stripping) due to the massive galaxies, the Galaxy and M 31 driving the evolutionary change between dwarf galaxy types.
- High Velocity Clouds (HVCs) are clouds of interstellar gas that are not associated with the Galaxy, and are probably infalling gas. Their origin is currently debated, though it is likely they are either remnant gas left over from the formation of the Galaxy, or they are associated with other galaxies that have been tidally disturbed due to the influence of the Galaxy.
- Despite containing 1% of the total Galaxy mass, the halo has provided clues to the earliest processes of formation. The halo forms from accreted satellite galaxies at ages > 10 Gyr ($z \sim 2$). The halo may not be homogeneous as recent observations suggest two distinct (inner, outer) components in which the outer component displays a net retrograde rotation signature and high velocity dispersion.
- The Galaxy disk has two distinct components. A thin disk of diameter of ~ 50 kpc, with a vertical scale height of 300 pc, and a $\sigma \sim 10$ km/s. A fainter, thick disk has a scale height some three times larger than the thin disk, of ~ 1 kpc, and a hotter dispersion of $\sigma \sim 40$ km/s.
- Under the Λ CDM paradigm formation of structure is hierarchically driven, with larger objects being built by the mergers of smaller objects. The building blocks will be dark matter halos with baryonic matter. A rapid mass assembly, and quiescent merging history (since $z \sim 2$, 10 Gyr ago) most likely explains the current observed properties of the Galaxy, though this is unusual in Λ CDM models.
- The Galaxy and M 31 will merge in 5.9 Gyr, after a first pericenter passage 3.9 Gyr from now, to ultimately resemble an elliptical galaxy.
- The LG has a velocity of $v_{LG} = 627 \pm 22$ km s $^{-1}$ with respect to the CMB. About 44% of the LG motion is due to the infall into the region of the Great Attractor, and the remaining amount of motion is due to more

distant overdensities between 130 and 180 h^{-1} Mpc, primarily the Shapley supercluster.

- The LG will continue towards the Virgo cluster, but never reach it. In the far future the LG will be isolated due to the accelerated expansion of the universe.

Additional reading

Advanced texts or papers are indicated with the † symbol.

J. Binney and M. Merrifield, 1998, *Galactic Astronomy*, (Princeton University Press, Princeton).

K. Freeman and J. Bland-Hawthorn, 2002, 'The New Galaxy: Signatures of Its Formation', *Annual Reviews of Astronomy and Astrophysics*, **40**, 487, also <http://arxiv.org/abs/astro-ph/0208106v1>

C.S. Frenk and S.D.M. White, 2012, *Annalen der Physik*, **524**, 507.

R.C. Kennicutt and N.J. Evans, 2012, 'Star Formation in the Milky Way and Nearby Galaxies', *Annual Reviews of Astronomy and Astrophysics*, **50**, 531, also <http://arxiv.org/abs/1204.3552v2>

M. Livio and T.M. Brown, 2006, *The Local Group as an Astrophysical Laboratory: Proceedings of the Space Telescope Science Institute Symposium*, (Cambridge University Press, Cambridge).

E. Tolstoy, V. Hill and M. Tosi, 2009, 'Star-Formation Histories, Abundances, and Kinematics of Dwarf Galaxies in the Local Group', *Annual Reviews of Astronomy and Astrophysics*, **47**, 371, also <http://www.astro.rug.nl/~etolstoy/tolstoyhilltosi09.pdf>

S. van den Bergh, 2000, *The Galaxies of the Local Group*, (Cambridge University Press, Cambridge).

Reference

A colour all-sky panorama image of the Galaxy. Credit: Mellinger (2009) <http://galaxy.phy.cmich.edu/~axel/mwpan2/krpano/>

Visualisations of the M 31-Galaxy merger process. Credit: van der Marel *et al.* (2012b) and NASA, ESA and F. Summers (STScI)

<http://hubblesite.org/newscenter/archive/releases/2012/20/video/j/>

http://www-int.stsci.edu/~marel/M31/M31_PaperIII_fig16c.mp4 (a 99 MB mp4 file)